

Lawrence Berkeley National Laboratory

LBL Publications

Title

VUV Photoionization Study of the Formation of the Simplest Polycyclic Aromatic Hydrocarbon: Naphthalene (C₁₀H₈)

Permalink

<https://escholarship.org/uc/item/3sv1m7pq>

Journal

The Journal of Physical Chemistry Letters, 9(10)

ISSN

1948-7185

Authors

Zhao, Long

Kaiser, Ralf I

Xu, Bo

et al.

Publication Date

2018-05-17

DOI

10.1021/acs.jpcelett.8b01020

Peer reviewed

A VUV Photoionization Study on the Formation of the Simplest Polycyclic Aromatic Hydrocarbon: Naphthalene (C₁₀H₈)

Long Zhao, Ralf I. Kaiser^{*,1}

Department of Chemistry, University of Hawaii at Manoa, Honolulu, Hawaii, 96822

Bo Xu, Utuq Ablikim, Musahid Ahmed^{*,2}

*Chemical Sciences Division, Lawrence Berkeley National Laboratory, Berkeley, California
94720*

Marsel V. Zagidullin and Valeriy N. Azyazov

*Samara National Research University, Samara 443086, Russia and
Lebedev Physical Institute, Samara 443011, Russia*

A. Hasan Howlader and Stanislaw F. Wnuk

*Department of Chemistry and Biochemistry, Florida International University, Miami, Florida
33199*

Alexander M. Mebel^{*,3}

*Department of Chemistry and Biochemistry, Florida International University, Miami, Florida
33199 and Samara National Research University, Samara 443086*

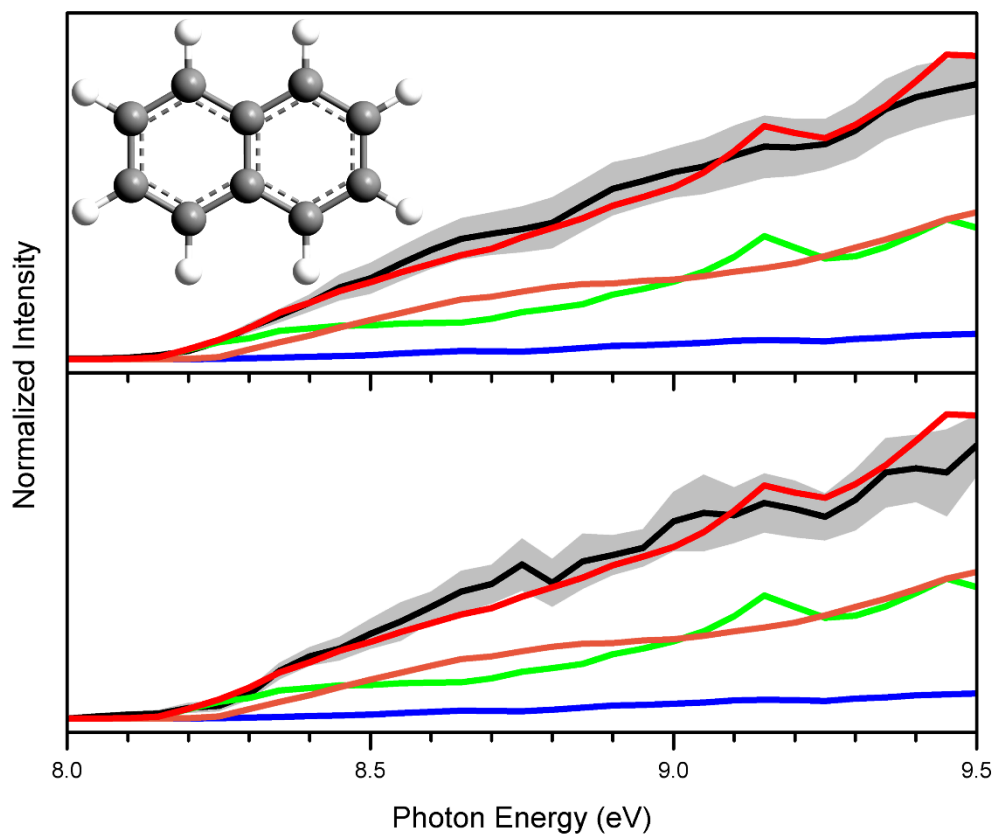
¹ E-mail: ralfk@hawaii.edu

² E-mail: mahmed@lbl.gov

³ E-mail: mebela@fiu.edu

ABSTRACT: The formation of the simplest polycyclic aromatic hydrocarbon (PAH) – naphthalene ($C_{10}H_8$) - was explored in a high-temperature chemical reactor under combustion-like conditions in the phenyl (C_6H_5) - vinylacetylene (C_4H_4) system. The products were probed utilizing tunable vacuum ultraviolet light by scanning the photoionization efficiency (PIE) curve at a mass-to-charge $m/z = 128$ ($C_{10}H_8^+$) of molecules entrained in a molecular beam. The data fitting with PIE reference curves of naphthalene, 4-phenylvinylacetylene ($C_6H_5CCC_2H_3$), and trans-1-phenylvinylacetylene ($C_6H_5CHCHCCH$) indicates that the isomers were generated with branching ratios of $43.5 \pm 9.0\% : 6.5 \pm 1.0\% : 50.0 \pm 10.0\%$. Kinetics simulations agree nicely with the experimental findings with naphthalene synthesized via the hydrogen abstraction – vinylacetylene addition (HAVA) pathway and through hydrogen-assisted isomerization of phenylvinylacetylenes. The HAVA route to naphthalene at elevated temperatures represents an alternative pathway to the hydrogen abstraction-acetylene addition (HACA) forming naphthalene in flames and circumstellar envelopes, whereas in cold molecular clouds, HAVA synthesizes naphthalene via a barrier-less bimolecular route.

TOC graphic



Polycyclic aromatic hydrocarbons (PAHs) – organic molecules consisting of fused benzene rings – along with their protonated, ionized, (de)hydrogenated, alkylated, and nitrogen-substituted counterparts have been proposed to carry up to 20% of the interstellar carbon budget. Inferred from the diffuse interstellar bands (DIBs)¹⁻² - discrete absorption features superimposed on the interstellar extinction curve covering the blue part of the visible spectrum (400 nm) to the near-infrared (1.2 μm) – and from the unidentified infrared (UIR) emission bands monitored from 3 to 14 μm ³⁻⁴, PAHs have been linked to the astrobiological evolution of the interstellar medium⁵ and are contemplated as key nucleation sites leading to carbonaceous dust particles (‘interstellar grains’)⁶⁻¹¹. Even though not a single PAH has been observed spectroscopically in the gas phase of the interstellar medium (ISM), the identification of the prototype PAH naphthalene (C_{10}H_8) along with higher-molecular weight PAHs like coronene ($\text{C}_{24}\text{H}_{12}$) in at least 20 carbonaceous chondrites proposes a circumstellar origin around envelopes of dying Asymptotic Giant Branch (AGB) stars¹²⁻¹³. State-of-the-art astrochemical models of PAH formation have been ‘borrowed’ from the combustion chemistry community with the most commended pathways to PAHs proposed to be associated with molecular weight growth processes via sequential reactions of resonantly stabilized (propargyl; C_3H_3) and also aromatic (phenyl; C_6H_5) radicals. Together with acetylene (C_2H_2), these reactions are contemplated as the foundation for the hydrogen abstraction - acetylene addition (HACA) mechanism¹⁴⁻¹⁹ driving PAH synthesis at elevated temperatures of up to a few 1,000 K. Supportive electronic structure calculations^{18,20-24} and kinetic modeling^{14,25-27} suggests that HACA involves a repetitive sequence of atomic hydrogen abstraction from the reacting aromatic hydrocarbon followed by sequential addition of two acetylene molecules to the radical sites prior to cyclization and aromatization^{12,15-16,20,26,28}.

However, in recent years, astronomical observations accompanied by astrochemical models revealed that interstellar PAHs are rapidly destroyed through interstellar shock waves and energetic galactic cosmic rays²⁹⁻³⁰ predicting life times of only a few 10^8 years. This contrasts the timescale for injection of new PAH-based material into the interstellar medium by AGB stars of typically 2×10^9 years. Consequently, the ubiquitous presence of PAHs in the extraterrestrial environments requires further pathways to a rapid formation of PAHs beyond the ‘established’ HACA route. Recently, Parker et al. revealed that naphthalene can be synthesized via the reaction of the phenyl radical (C_6H_5) with vinylacetylene (C_4H_4) via the hydrogen abstraction – vinylacetylene addition (HAVA) reaction pathway. This bimolecular reaction was found to be de-facto barrier-less and leads via a single, bimolecular gas phase

collision to naphthalene ($C_{10}H_8$) plus atomic hydrogen at temperatures as low as 10 K³¹. However, the phenyl – vinylacetylene system has not been explored at elevated temperatures relevant to circumstellar envelopes of carbon stars of a few 1,000 K or under combustion-like conditions reaching up to 2,000 K. Here, the reaction mechanism and branching ratios of the isomers can be quite distinct from 10 K due to a much larger entropy factor and alternative addition routes of the phenyl radical to the carbon atoms of vinylacetylene, which involve entrance barriers. These pathways might be competitive at high temperatures and may lead to non-naphthalene isomers such as phenylvinylacetylenes thus potentially reducing the yield of naphthalene.

In this *Letter*, we expose that the aromatic naphthalene molecule can be synthesized via the reaction of pyrolytically generated phenyl radicals (C_6H_5) with vinylacetylene ($HCCCHCH_2$; C_4H_4) at elevated temperatures of 1,600 K via resonantly stabilized $C_{10}H_{11}$ reaction intermediates exploiting a high-temperature chemical reactor. For distinct structural isomers such as naphthalene and azulene the adiabatic ionization energies along with the corresponding photoionization efficiency curves (PIEs), which report the intensity of the ion counts at $m/z = 128$ ($C_{10}H_8^+$) versus the photon energy, are distinct. Therefore, by photoionizing the neutral $C_{10}H_8$ products in a molecular beam by tunable vacuum ultraviolet light (VUV) from the Advanced Light Source (ALS) at various photon energies, we extracted the PIE curve of $C_{10}H_8^+$ at $m/z = 128$. Through a comparison of this experimentally recorded PIE curves with a linear combination of known reference PIE curves for various $C_{10}H_8$ isomers, naphthalene, 4-phenylvinylacetylene, and trans-1-phenylvinylacetylene were found to represent the $C_{10}H_8$ isomers synthesized in the reaction of the phenyl radical with vinylacetylene.

Figures 1 and 2 reveal the mass spectra of the species ionized in the supersonic expansion along with the PIE curve of $m/z = 128$ ($C_{10}H_8^+$) recorded in phenyl – vinyl-acetylene system. Figure 2 exhibits the data over a range of photon energies from 8.0 to 9.5 eV along with the PIE reference curves of naphthalene and 4- and trans-1-phenylvinylacetylene, together with the overall fit. These data document an excellent match of the experimentally recorded PIE curve at $m/z = 128$ with a linear combination of the reference curves of three $C_{10}H_8$ isomers. The onset of the ion counts at 8.10 eV agrees exceptionally well with the adiabatic ionization energy of naphthalene of 8.12 eV,³² whereas the contributions of the additional isomers, especially 4-phenylvinylacetylene, become apparent around 8.25 eV. The branching ratios for naphthalene to trans-1-phenylvinylacetylene to 4-phenylvinylacetylene were calculated based

on the overall fitting of the experimental PIE curve at $m/z = 128$. All the PIE calibration curves for naphthalene, trans-1-phenylvinylacetylene and 4-phenylvinylacetylene were newly measured in this work, with the photoionization cross sections at 9.5 eV being 23.7 Mb, 30.2 Mb, and 23.0 Mb, respectively. By linear fitting of these calibration PIE curves to the experimentally measured curve, the branching ratios were extracted to be $43.5 \pm 9.0\%$: $6.5 \pm 1.0\%$: $50.0 \pm 10.0\%$, taking 20% uncertainty in the PIE curves into consideration. It should be noted that the other two-ring $C_{10}H_8$ isomer, azulene, has an ionization threshold of 7.42 eV³² and therefore the absence of ionization signal below 8.14 eV clearly indicates the absence of azulene as a reaction product. Also, it is important to highlight that under our experimental conditions, the nitrosobenzene precursor (C_6H_5NO ; 107 amu), which is present at a level of 2.6% in the helium-seeded vinylacetylene (5%) beam, decomposes *quantitatively* to the phenyl radical (C_6H_5) plus nitrogen monoxide (NO).^{15,33-35} Likewise, control experiments in the absence of vinylacetylene do not depict any signal at $m/z = 128$.³³ Therefore, we conclude that the formation of naphthalene and its isomers requires the presence of the phenyl radical *and* vinylacetylene in the reactor (Supporting Information).

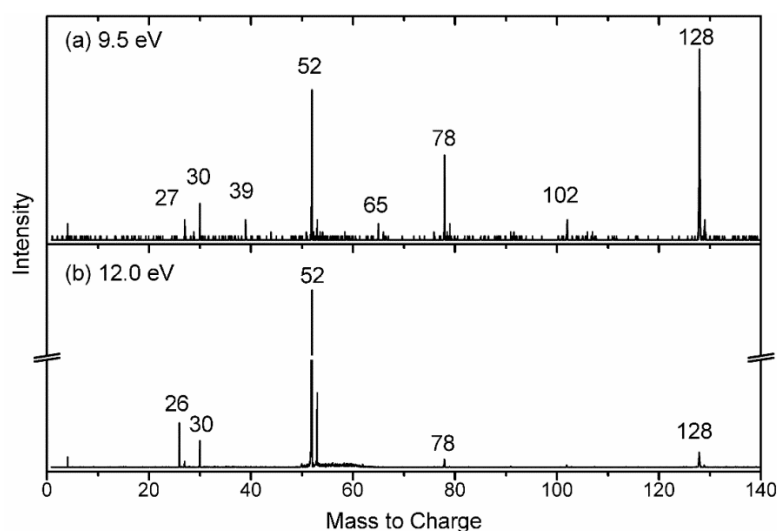


Figure 1. Mass spectra of species in the helium-seeded supersonic beam recorded at photon energies of 9.5 eV (a) and 12.0 eV (b). Products beyond the $C_{10}H_8$ isomers naphthalene, trans-1-phenylvinylacetylene, and 4-phenylvinylacetylene are discussed in the Supporting Information.

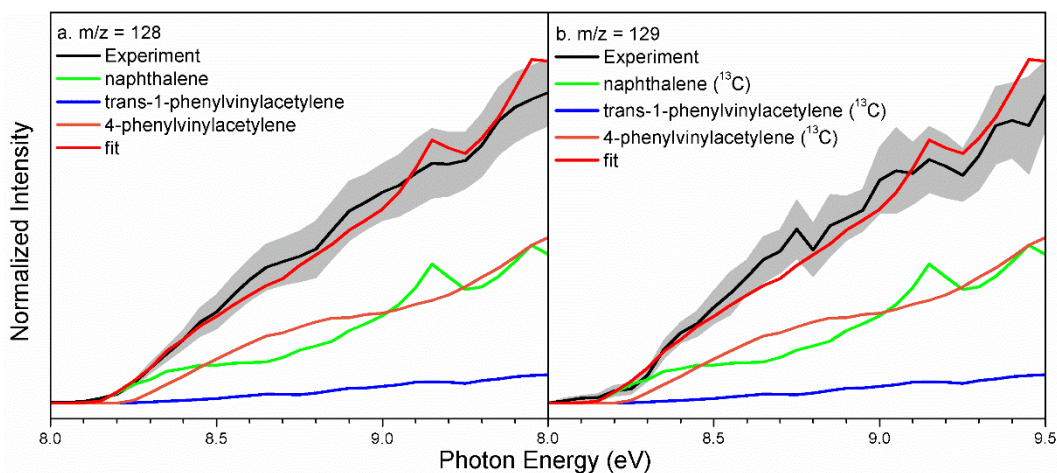


Figure 2. Experimental and reference PIE curves for species at $m/z = 128$ (a) and 129 (b) in the phenyl-vinylacetylene system. The black line refers to the normalized experimental data with 1σ error limits defined in the shaded area; the green, orange, and blue lines show the isomer PIE curves generated by linear fit with measured references PIE curves of naphthalene, 4-phenylvinylacetylene and trans-1-phenylvinylacetylene, respectively. The red line reveals the overall fit via a linear combination of the reference curves.

Having identified naphthalene, 4-phenylvinylacetylene, and trans-1-phenylvinylacetylene, we are also aiming to elucidate the underlying reaction pathway(s). This requires a close look at the pertinent potential energy surfaces (PES) and also simulation of the gas flow inside the pyrolytic reactor using the COMSOL package coupled with a kinetics model accounting for the residence time in the heated micro reactor of about $560 \mu\text{s}$ (Supporting Information). Our recent theoretical study³⁶ described the PES for the reaction, structures and molecular properties of all intermediates and transition states involved, and temperature- and pressure-dependent rate constants in the phenyl–vinylacetylene system. The results of the kinetics calculations revealed that under the experimental conditions of the reactor, the prevailing products are 4-phenylvinylacetylene (P3) and trans-1-phenylvinylacetylene (P2) along with atomic hydrogen with rate constants of $1.4 \times 10^{-12} \text{ cm}^3 \text{ molecule}^{-1} \text{ s}^{-1}$ and $6.6 \times 10^{-13} \text{ cm}^3 \text{ molecule}^{-1} \text{ s}^{-1}$ and yields - excluding the direct hydrogen abstraction products - of 62 % and 31 %, respectively. The yields of naphthalene (P1) were computed to be less than 1% with the rate constant for its formation as low as $1.3 \times 10^{-14} \text{ cm}^3 \text{ molecule}^{-1} \text{ s}^{-1}$. Here, 4-phenylvinylacetylene is produced via the phenyl radical addition to the C4 acetylenic carbon atom occurring via a barrier of 5 kJ mol^{-1} followed by the atomic hydrogen loss from the attacked carbon atom (Figure 3). Similarly, trans-1-phenylvinylacetylene is formed by phenyl addition to the C1

carbon atom of the vinyl moiety via a submerged barrier located 0.4 kJ mol^{-1} below the reactants. It is important to note that the pathway to naphthalene proceeds through the same submerged barrier and involves two hydrogen shifts and ring closure prior to hydrogen atom elimination; the transition state is lower in energy than the barrier involved in the immediate hydrogen atom loss from the collision complex forming trans-1-phenylvinylacetylene. Consequently, the pathway to naphthalene is favorable at low temperatures and pressures. However, this channel does not appear to be competitive at 1,600 K in our reactor due to the unfavorable entropic factor. In addition to the C_{10}H_8 products, the formation of the direct hydrogen atom abstraction products benzene (C_6H_6) along with distinct C_4H_3 isomers is competitive at 1,600 K with rate constants of 5.8×10^{-13} and $3.8 \times 10^{-13} \text{ cm}^3 \text{ molecule}^{-1} \text{ s}^{-1}$ for *i*- C_4H_3 and *n*- C_4H_3 , respectively.

How can we explain the predominant formation of naphthalene in the pyrolytic reactor? The aforementioned discussion only accounted for bimolecular collisions and hence the primary reaction products. However, the pressure profile in the reactor, the presence of hydrogen atoms released in the bimolecular reactions, and the residence time also allows for secondary reactions to occur (Supporting Information). Therefore, a detailed kinetic modeling coupled with the gas flow simulations allows us to reconcile theory and experiment. This model is essential to extract the dominating reactions in the reactor since the conditions such as temperature and pressure along the reactor axis are not homogeneous (Supporting Information). The kinetic reaction scheme includes the quantitative unimolecular decomposition of the reactants such as nitrosobenzene ($\text{C}_6\text{H}_5\text{NO}$), the primary reactions of the phenyl radical (C_6H_5) with vinylacetylene (C_4H_4), secondary reactions of the hydrogen assisted isomerization of the C_{10}H_8 isomers, and reactions to account for the detection of acetylene (C_2H_2 , $m/z = 26$), the vinyl radical (C_2H_3 , $m/z = 27$), the propargyl radical (C_3H_3 , $m/z = 39$), cyclopentadienyl (C_5H_5 , $m/z = 65$), benzene and fulvene (C_6H_6 , $m/z = 78$), and phenylacetylene (C_8H_6 , $m/z = 102$) with rate constants extracted taken from the literature (Supporting Information).³⁶⁻⁵⁰ Figure 4 illustrates the overall change of the concentration of phenyl (C_6H_5), benzene (C_6H_6), and the C_{10}H_8 isomers along the reactor axis. Considering the pyrolysis, the fraction of the phenyl radical manifests a fast growth and rapid drop peaking at the distance where the gas temperature is close to 1,100 K. The interval required for the quantitative nitrosobenzene ($\text{C}_6\text{H}_5\text{NO}$) decomposition along the axis is only 1 mm. From this point, the phenyl radicals start producing initial C_{10}H_8 isomers via primary reactions. During the distance from about 1.2 cm to 1.5 cm, the fractions of the phenylvinylacetylene isomers (P2, P3) grow much faster than that for

naphthalene (P1). Later, P2 and P3 convert to the most stable naphthalene isomer via hydrogen assisted isomerization (R4) and (R5) (Supporting Information). The transformation of P2 and P3 into P1 occurs in the distances from 1.5 cm to 2.0 cm and essentially terminates at a distance of 2.0 cm from the entrance of the microreactor. The calculated and experimental molar fractions of P1, P2, and P3 at the exit of the microreactor showed that the experimental conditions are not favorable for the total transformation of P2 and P3 into P1. The incomplete transformation of P2 and P3 into P1 is based on several factors, including a low rate constant of reaction (R5c), a sharp drop of the hydrogen atoms concentration, and the short length of the reactor. Kinetic simulations revealed that a nearly total transformation of P2 and P3 into P1 can be achieved at times larger 10 ms. This order of magnitude is much larger than the residence time in our reactor. This emphasizes the advantage of the short-length microreactor allowing us to reveal fine details of the elementary reaction mechanism (primary and secondary reactions), which otherwise would have been masked due to the full conversion of all C₁₀H₈ isomers produced initially to naphthalene.

To summarize, our experiments exploiting a high-temperature chemical reactor revealed that the simplest polycyclic aromatic hydrocarbon - naphthalene (C₁₀H₈) - can be synthesized under combustion-like conditions via a directed synthesis of the phenyl radical reacting with vinylacetylene. Higher energy structural isomers of naphthalene - trans-1-phenylvinylacetylene and 4-phenylvinylacetylene - which also form in the reactor, undergo hydrogen-assisted isomerization to the thermodynamically most stable naphthalene molecule during their residence time in the reactor. These pathways are strongly distinct from crossed molecular beams studies of this system,³¹ in which the nascent reaction products ‘fly away’ from the reaction center and, hence, cannot undergo subsequent hydrogen assisted isomerization reactions. Therefore, crossed molecular beams and pyrolytic reactor studies are highly complementary leading to the identification of polycyclic aromatic hydrocarbons (naphthalene) along with high energy isomers synthesized under single collision conditions (crossed beams) together with hydrogen-assisted isomerization products (pyrolytic reactor) ultimately untangling the complex processes and reaction mechanisms of elementary bimolecular reactions leading to PAHs in combustion systems and in extraterrestrial environments. Further, the combined gas flow and kinetic simulations of the reactor resemble a powerful tool not only for a detailed understanding of the intricate physical and chemical processes inside the high-temperature chemical reactor, but also for a quantification and validation of the observed product yields. Future studies of this reactor in combination with electronic structure calculations and kinetics

simulations are aimed to systematically unravel mass growth processes via aryl-type radical reactions with acetylene (HACA) and vinylacetylene (HAVA) synthesizing three- and even four-membered PAHs such as anthracene, phenanthrene, and triphenylene. However, whereas PAH formation via HACA only operates at elevated temperatures due to the inherent barriers of aryl radical addition to acetylene, HAVA may operate at temperatures as low as 10 K as well considering the de-facto barrierless nature of this mechanism. In particular, at very low pressures and in the temperature range of 100-200 K, the rate constant for $C_6H_5 + C_4H_4 \rightarrow$ naphthalene + H, $4-6 \times 10^{-15} \text{ cm}^3 \text{ molecule}^{-1} \text{ s}^{-1}$ is from eight to two orders of magnitude higher than the rate constant for $C_6H_5 + C_2H_2 \rightarrow$ phenylacetylene + H, the first step in HACA, and the difference is even higher below 100 K. This can lead to the formation of distinct PAHs in cold molecular clouds via HAVA, which cannot be synthesized via HACA-type mechanisms thus providing an intimate understanding of the carbon chemistry in the universe.

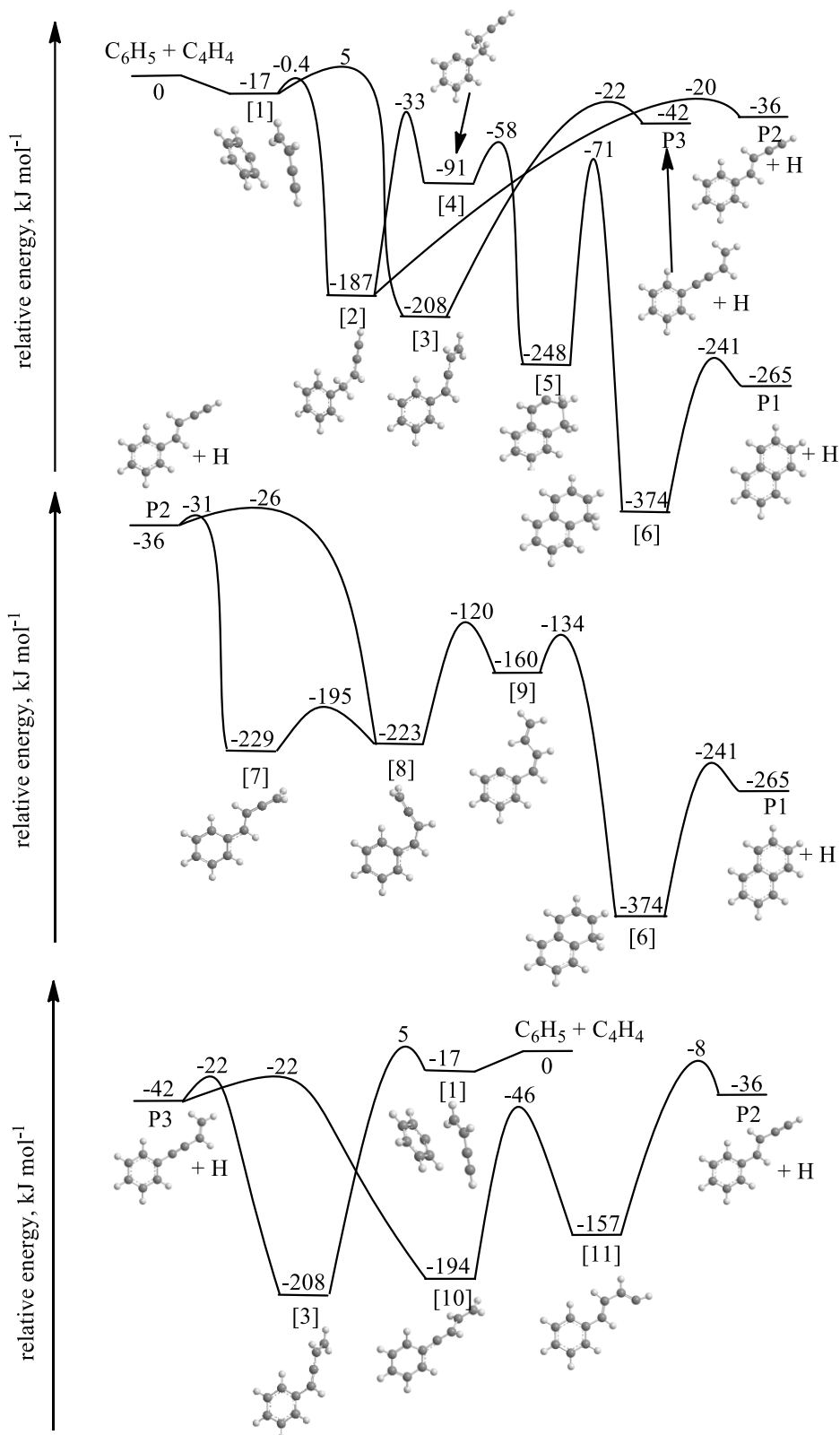


Figure 3. Potential energy surfaces (PES) for the most favorable channels involved in the formation of three C₁₀H₈ isomers within the phenyl – vinylacetylene system via bimolecular

reactions (top) and hydrogen assisted isomerization (center, bottom) based on the calculations from Ref. ³⁶.

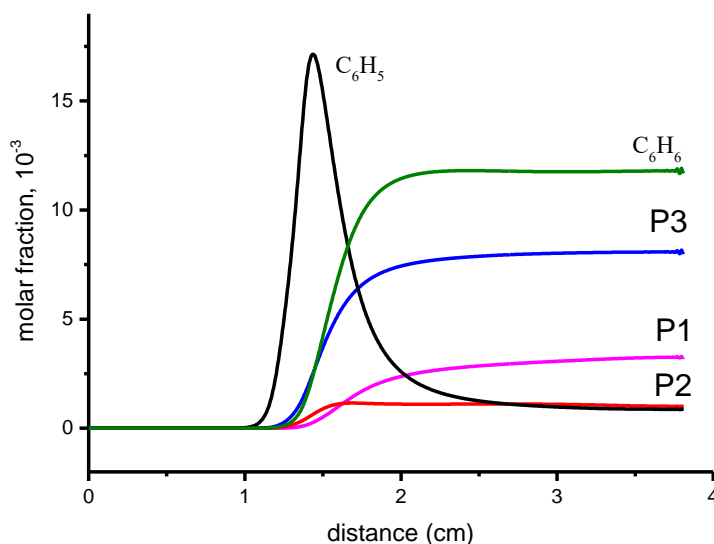


Figure 4. Simulated profiles of the molar fractions of phenyl (C_6H_5), benzene (C_6H_6), and the $C_{10}H_8$ isomers naphthalene (P1), trans-1-phenylvinylacetylene (P2), and 4-phenylvinylacetylene (P3) along the reactor axis.

Experimental Method

The experiments were conducted at the Advanced Light Source (ALS) at the Chemical Dynamics Beamline (9.0.2.) exploiting a high-temperature chemical reactor. Briefly, the reactor consists of a resistively heated silicon carbide (SiC) tube of 20 mm length and 1 mm inner diameter. A continuous supersonic beam of phenyl radicals (C_6H_5) was generated *in situ* via quantitative pyrolysis of nitrosobenzene (C_6H_5NO , TCI-America, > 98 %, 323 K) seeded in vinylacetylene/helium carrier gas (5% C_4H_4 in He; Airgas) introduced at a backing pressure of 300 Torr and 1,600 K into the silicon carbide tube. Vinylacetylene does not only act as a seeding gas, but also as a reactant with the phenyl radical. The residence time of the reactants in the reactor was determined to be near 560 μs (Supporting Information). After exiting the silicon carbide tube, the molecular beam, which contains the reaction products, passes a 2 mm skimmer and enters the detection chamber containing a Wiley-McLaren reflectron time-of-flight (ReTOF) mass spectrometer. The products were then photoionized in the extraction region of the ReTOF by exploiting quasi-continuous tunable vacuum ultraviolet (VUV) synchrotron light and detected with a microchannel plate (MCP). Here, mass spectra were taken

in the photon energy range from 8.00 eV to 9.50 eV in steps of 0.05 eV. The photoionization efficiency (PIE) curves, which report the intensity of a single mass-to-charge ratio (m/z) versus the photon energy, were extracted by integrating the signal collected at a specific m/z selected for the species of interest over the range of photon energies and normalized to the incident photon flux. The supersonically cooled nature of the beam of the product molecules presents a crucial prerequisite for their detection since the products are rotationally and vibrationally cooled in the expansion⁵¹. Two naphthalene isomers - 4-phenylvinylacetylene (P3) and trans-1-phenylvinylacetylene (P2) - were synthesized by Sonogashira cross-coupling reactions (Supporting Information); their PIE curves were recorded via vacuum sublimation of these isomers, recording mass spectra from 8.00 eV to 9.50 eV in steps of 0.05 eV, and extracting the ion count profiles at $m/z = 128$.

Supporting Information Available: Description of the synthesis of 4-phenylvinylacetylene and trans-1-phenylvinylacetylene including ¹H NMR and ¹³C NMR spectra of these compounds; description of the modeling procedure of the gas flow and kinetics of the phenyl – vinylacetylene system in the microreactor including the reaction mechanism, physical constants, and reaction rate constants used; PIE curves and fits of low molecular weight products.

Acknowledgements

This work was supported by the US Department of Energy, Basic Energy Sciences DE-FG02-03ER15411 and DE-FG02-04ER15570 to the University of Hawaii and to Florida International University, respectively. M.A. along with the Advanced Light Source are supported by the Director, Office of Science, Office of Basic Energy Sciences, of the U.S. Department of Energy under Contract No. DE-AC02-05CH11231, through the Chemical Sciences Division. The reactor modeling studies at Samara National Research University were supported by Ministry of Education and Science of the Russian Federation (Grant No. 14.Y26.31.0020). H.H. is recipient of the Florida International University Presidential Fellowship. The authors thank Dr. Stephen J. Klippenstein for sharing with us some unpublished rate constants related to reactions on C₄H₅ (H + C₄H₄), C₆H₆, and C₆H₇ (C₄H₅ + C₂H₂) potential energy surfaces used in kinetic modeling.

References

1. Salama, F.; Galazutdinov, G.; Krelowski, J.; Allamandola, L.; Musaev, F., Polycyclic Aromatic Hydrocarbons and the Diffuse Interstellar Bands: A Survey. *Astrophys. J.* **1999**, *526*, 265-273.
2. Duley, W., Polycyclic Aromatic Hydrocarbons, Carbon Nanoparticles and the Diffuse Interstellar Bands. *Faraday Discuss.* **2006**, *133*, 415-425.
3. Ricks, A. M.; Douberly, G. E.; Duncan, M. A., The Infrared Spectrum of Protonated Naphthalene and Its Relevance for the Unidentified Infrared Bands. *Astrophys. J.* **2009**, *702*, 301-306.
4. Schlemmer, S.; Cook, D.; Harrison, J.; Wurfel, B.; Chapman, W.; Saykally, R., The Unidentified Interstellar Infrared Bands: PAHs as Carriers? *Science* **1994**, *265*, 1686-1689.
5. Bernstein, M. P.; Sandford, S. A.; Allamandola, L. J.; Gillette, J. S.; Clemett, S. J.; Zare, R. N., UV Irradiation of Polycyclic Aromatic Hydrocarbons in Ices: Production of Alcohols, Quinones, and Ethers. *Science* **1999**, *283*, 1135-1138.
6. Ehrenfreund, P.; Sephton, M. A., Carbon Molecules in Space: From Astrochemistry to Astrobiology. *Faraday Discuss.* **2006**, *133*, 277-288.
7. Herbst, E.; Van Dishoeck, E. F., Complex Organic Interstellar Molecules. *Annu. Rev. Astron. Astrophys.* **2009**, *47*, 427-480.
8. Puget, J. L.; Léger, A., A New Component of the Interstellar Matter: Small Grains and Large Aromatic Molecules. *Annu. Rev. Astron. Astrophys.* **1989**, *27*, 161-198.
9. Schmitt-Kopplin, P.; Gabelica, Z.; Gougeon, R. D.; Fekete, A.; Kanawati, B.; Harir, M.; Gebefuegi, I.; Eckel, G.; Hertkorn, N., High Molecular Diversity of Extraterrestrial Organic Matter in Murchison Meteorite Revealed 40 Years after Its Fall. *Proc. Natl. Acad. Sci. U.S.A.* **2010**, *107*, 2763-2768.
10. Tielens, A. G. G. M., Interstellar Polycyclic Aromatic Hydrocarbon Molecules. *Annu. Rev. Astron. Astrophys.* **2008**, *46*, 289-337.
11. Ziurys, L. M., The Chemistry in Circumstellar Envelopes of Evolved Stars: Following the Origin of the Elements to the Origin of Life. *Proc. Natl. Acad. Sci. U.S.A.* **2006**, *103*, 12274-12279.
12. Frenklach, M.; Feigelson, E. D., Formation of Polycyclic Aromatic Hydrocarbons in Circumstellar Envelopes. *Astrophys. J.* **1989**, *341*, 372-384.
13. Cherchneff, I., The Inner Wind of IRC+ 10216 Revisited: New Exotic Chemistry and Diagnostic for Dust Condensation in Carbon Stars. *A & A* **2012**, *545*, A12/1-A12/14.
14. Wang, H.; Frenklach, M., A Detailed Kinetic Modeling Study of Aromatics Formation in Laminar Premixed Acetylene and Ethylene Flames. *Combust. Flame* **1997**, *110*, 173-221.
15. Parker, D. S.; Kaiser, R. I.; Troy, T. P.; Ahmed, M., Hydrogen Abstraction/Acetylene Addition Revealed. *Angew. Chem. Int. Ed.* **2014**, *53*, 7740-7744.
16. Parker, D. S. N.; Kaiser, R. I.; Bandyopadhyay, B.; Kostko, O.; Troy, T. P.; Ahmed, M., Unexpected Chemistry from the Reaction of Naphthyl and Acetylene at Combustion-Like Temperatures. *Angew. Chem. Int. Ed.* **2015**, *54*, 5421-5424.
17. Parker, D. S. N.; Kaiser, R. I.; Kostko, O.; Ahmed, M., Selective Formation of Indene through the Reaction of Benzyl Radicals with Acetylene. *ChemPhysChem* **2015**, *16*, 2091-2093.
18. Yang, T.; Kaiser, R. I.; Troy, T. P.; Xu, B.; Kostko, O.; Ahmed, M.; Mebel, A. M.; Zagidullin, M. V.; Azyazov, V. N., HACA's Heritage: A Free-Radical Pathway to Phenanthrene in Circumstellar Envelopes of Asymptotic Giant Branch Stars. *Angew. Chem. Int. Ed.* **2017**, *56*, 4515-4519.
19. Matsugi, A.; Miyoshi, A., Modeling of Two- and Three-Ring Aromatics Formation in the Pyrolysis of Toluene. *Proc. Combust. Inst.* **2013**, *34*, 269-277.
20. Richter, H.; Howard, J. B., Formation of Polycyclic Aromatic Hydrocarbons and Their Growth to Soot - A Review of Chemical Reaction Pathways. *Prog. Energy Combust. Sci.* **2000**, *26*, 565-608.
21. Marsh, N. D.; Wornat, M. J., Formation Pathways of Ethynyl-Substituted and Cyclopenta-Fused Polycyclic Aromatic Hydrocarbons. *Proc. Combust. Inst.* **2000**, *28*, 2585-2592.
22. Tokmakov, I.; Lin, M., Reaction of Phenyl Radicals with Acetylene: Quantum Chemical Investigation of the Mechanism and Master Equation Analysis of the Kinetics. *J. Am. Chem. Soc.* **2003**, *125*, 11397-11408.
23. Kislov, V.; Islamova, N.; Kolker, A.; Lin, S.; Mebel, A., Hydrogen Abstraction Acetylene Addition and Diels-Alder Mechanisms of PAH Formation: A Detailed Study Using First Principles Calculations. *J. Chem. Theory Comput.* **2005**, *1*, 908-924.

24. Kislov, V.; Sadovnikov, A.; Mebel, A., Formation Mechanism of Polycyclic Aromatic Hydrocarbons beyond the Second Aromatic Ring. *J. Phys. Chem. A* **2013**, *117*, 4794-4816.
25. Frenklach, M.; Wang, H., Detailed Modeling of Soot Particle Nucleation and Growth. *Proc. Combust. Inst.* **1991**, *23*, 1559-1566.
26. Bittner, J.; Howard, J., Composition Profiles and Reaction Mechanisms in a Near-Sooting Premixed Benzene/Oxygen/Argon Flame. *Proc. Combust. Inst.* **1981**, *18*, 1105-1116.
27. Wang, H.; Frenklach, M., Calculations of Rate Coefficients for the Chemically Activated Reactions of Acetylene with Vinylic and Aromatic Radicals. *J. Phys. Chem.* **1994**, *98*, 11465-11489.
28. Appel, J.; Bockhorn, H.; Frenklach, M., Kinetic Modeling of Soot Formation with Detailed Chemistry and Physics: Laminar Premixed Flames of C₂ Hydrocarbons. *Combust. Flame* **2000**, *121*, 122-136.
29. Micelotta, E.; Jones, A.; Tielens, A., Polycyclic Aromatic Hydrocarbon Processing in Interstellar Shocks. *A & A* **2010**, *510*, A36/1-A36/19.
30. Jones, A.; Nuth, J., Dust Destruction in the ISM: A Re-Evaluation of Dust Lifetimes. *A & A* **2011**, *530*, A44/1-A44/12.
31. Parker, D. S.; Zhang, F.; Kim, Y. S.; Kaiser, R. I.; Landera, A.; Kislov, V. V.; Mebel, A. M.; Tielens, A., Low Temperature Formation of Naphthalene and Its Role in the Synthesis of PAHs (Polycyclic Aromatic Hydrocarbons) in the Interstellar Medium. *Proc. Natl. Acad. Sci. U.S.A.* **2012**, *109*, 53-58.
32. Jochims, H. W.; Rasekh, H.; Ruehl, E.; Baumgaertel, H.; Leach, S., The Photofragmentation of Naphthalene and Azulene Monocations in the Energy Range 7-22 eV. *Chem. Phys.* **1992**, *168*, 159-84.
33. Zhang, F.; Kaiser, R. I.; Kislov, V. V.; Mebel, A. M.; Golan, A.; Ahmed, M., A VUV Photoionization Study of the Formation of the Indene Molecule and Its Isomers. *J. Phys. Chem. Lett.* **2011**, *2*, 1731-1735.
34. Zhang, F.; Kaiser, R. I.; Golan, A.; Ahmed, M.; Hansen, N., A VUV Photoionization Study of the Combustion-Relevant Reaction of the Phenyl Radical (C₆H₅) with Propylene (C₃H₆) in a High Temperature Chemical Reactor. *J. Phys. Chem. A* **2012**, *116*, 3541-3546.
35. Golan, A.; Ahmed, M.; Mebel, A. M.; Kaiser, R. I., A VUV Photoionization Study of the Multichannel Reaction of Phenyl Radicals with 1,3-Butadiene under Combustion Relevant Conditions. *Phys. Chem. Chem. Phys.* **2013**, *15*, 341-347.
36. Mebel, A. M.; Landera, A.; Kaiser, R. I., Formation Mechanisms of Naphthalene and Indene: From the Interstellar Medium to Combustion Flames. *J. Phys. Chem. A* **2017**, *121*, 901-926.
37. Park, J.; Dyakov, I.; Mebel, A.; Lin, M., Experimental and Theoretical Studies of the Unimolecular Decomposition of Nitrosobenzene: High-Pressure Rate Constants and the C–N Bond Strength. *J. Phys. Chem. A* **1997**, *101*, 6043-6047.
38. Horn, C.; Frank, P.; Tranter, R. S.; Schaugg, J.; Grotheer, H.-H.; Just, T., Direct Measurement of the Reaction Pair C₆H₅NO → C₆H₅ + NO by a Combined Shock Tube and Flow Reactor Approach. *Proc. Combust. Inst.* **1996**, *26*, 575-582.
39. Zador, J.; Fellows, M. D.; Miller, J. A., Initiation Reactions in Acetylene Pyrolysis. *J. Phys. Chem. A* **2017**, *121*, 4203-4217.
40. Mebel, A. M.; Georgievskii, Y.; Jasper, A. W.; Klippenstein, S. J., Temperature- and Pressure-Dependent Rate Coefficients for the HACA Pathways from Benzene to Naphthalene. *Proc. Combust. Inst.* **2017**, *36*, 919-926.
41. Miller, J. A.; Klippenstein, S. J.; Robertson, S. H., A Theoretical Analysis of the Reaction Between Vinyl and Acetylene: Quantum Chemistry and Solution of the Master Equation. *J. Phys. Chem. A* **2000**, *104*, 7525-7536.
42. Knyazev, V. D.; Slagle, I. R., Experimental and Theoretical Study of The C₂H₃ ⇌ H + C₂H₂ Reaction. Tunneling and the Shape of Falloff Curves. *J. Phys. Chem.* **1996**, *100*, 16899-16911.
43. Bauich, D.; Cobos, C.; Cox, C.; Esser, C.; Frank, P.; Just, T.; Kerr, J.; Pilling, M.; Troe, J.; Walker, R., Evaluated Kinetic Data for Combustion Modelling. *J. Phys. Chem. Ref. Data* **1992**, *21*, 411-429.
44. Harding, L. B.; Georgievskii, Y.; Klippenstein, S. J., Predictive Theory for Hydrogen Atom–Hydrocarbon Radical Association Kinetics. *J. Phys. Chem. A* **2005**, *109*, 4646-4656.
45. Miller, J. A.; Klippenstein, S. J., The Recombination of Propargyl Radicals and Other Reactions on a C₆H₆ Potential. *J. Phys. Chem. A* **2003**, *107*, 7783-7799.

46. Semenikhin, A.; Savchenkova, A.; Chechet, I.; Matveev, S.; Liu, Z.; Frenklach, M.; Mebel, A., Rate Constants for H Abstraction from Benzo(a)pyrene and Chrysene: A Theoretical Study. *Phys. Chem. Chem. Phys.* **2017**, *19*, 25401-25413.
47. Jasper, A. W.; Hansen, N., Hydrogen-Assisted Isomerizations of Fulvene to Benzene and of Larger Cyclic Aromatic Hydrocarbons. *Proc. Combust. Inst.* **2013**, *34*, 279-287.
48. da Silva, G., Mystery of 1-Vinylpropargyl Formation from Acetylene Addition to the Propargyl Radical: An Open-and-Shut Case. *J. Phys. Chem. A* **2017**, *121*, 2086-2095.
49. Madden, L.; Moskaleva, L.; Kristyan, S.; Lin, M., Ab Initio MO Study of the Unimolecular Decomposition of the Phenyl Radical. *J. Phys. Chem. A* **1997**, *101*, 6790-6797.
50. Senosiain, J. P.; Miller, J. A., The Reaction of *n*- and *i*-C₄H₅ Radicals with Acetylene. *J. Phys. Chem. A* **2007**, *111*, 3740-3747.
51. Vasiliou, A. K.; Piech, K. M.; Reed, B.; Zhang, X.; Nimlos, M. R.; Ahmed, M.; Golan, A.; Kostko, O.; Osborn, D. L.; David, D. E., Thermal Decomposition of CH₃CHO Studied by Matrix Infrared Spectroscopy and Photoionization Mass Spectroscopy. *J. Chem. Phys.* **2012**, *137*, 164308/1-164308/14.

Materials & Methods

Experiments were carried out at the Chemical Dynamics Beamline (9.0.2) of the Advanced Light Source in the Lawrence Berkeley National Laboratory. Employing a resistively-heating high-temperature silicon carbide (SiC) tube (chemical reactor), the molecular beam apparatus is equipped with a Wiley-McLaren Reflectron Time-of-Flight Mass Spectrometer (Re-TOF-MS). The chemical reactor mimics combustion-like conditions such as temperature and pressure along with chemical reactions to synthesize PAHs *in situ* involving reactions of combustion-relevant radicals. Here, styrenyl or *ortho*-vinylphenyl radicals (C_8H_7) were generated *in situ* via pyrolysis of β -bromostyrene or 2-bromostyrene (C_8H_7Br ; Sigma Aldrich) seeded in neat acetylene or helium gases of 400 Torr in a temperature of $1,500 \pm 50$ K, respectively. The concentrations of β -boromostyrene/2-bromostyrene in acetylene/helium were estimated to be less than 0.1% with residence time of a few tens of microseconds.^[1-2] The temperature of the SiC tube was monitored using a Type-C thermocouple. The acetylene gas did not only act as a carrier gas, but also as a reactant with the pyrolytically generated radicals. Reaction products generated in the reactor were expanded supersonically and passed through a 2 mm diameter skimmer located 10 mm downstream and into the main chamber which houses the Re-TOF-MS. The quasi-continuous tunable vacuum ultraviolet (VUV) light from the Advanced Light Source intercepted the neutral molecular beam in the extraction region of a Wiley–McLaren Re-TOF-MS. VUV single photon ionization profits from fragment-free ionization and hence is defined as a soft ionization method in contrast to electron impact ionization, which often results in excessive fragmentation of the parent ion. The ions formed via photoionization were then extracted perpendicularly to the molecular beam and fed into a microchannel plate detector by an ion lens. Photoionization efficiency (PIE) curves, which report ion counts as a function of photon energy at a particular mass-to-charge ratio (m/z), were extracted by integrating the signal recorded at the specific m/z over the energy range 8.00 eV to 11.00 eV in an increment of 0.05 eV and normalized to the photon flux. We also conducted blank experiments by expanding only acetylene carrier gas into the resistively-heated SiC tube and by replacing acetylene with helium carrier gas. No naphthalene reaction products were detected in these control experiments.

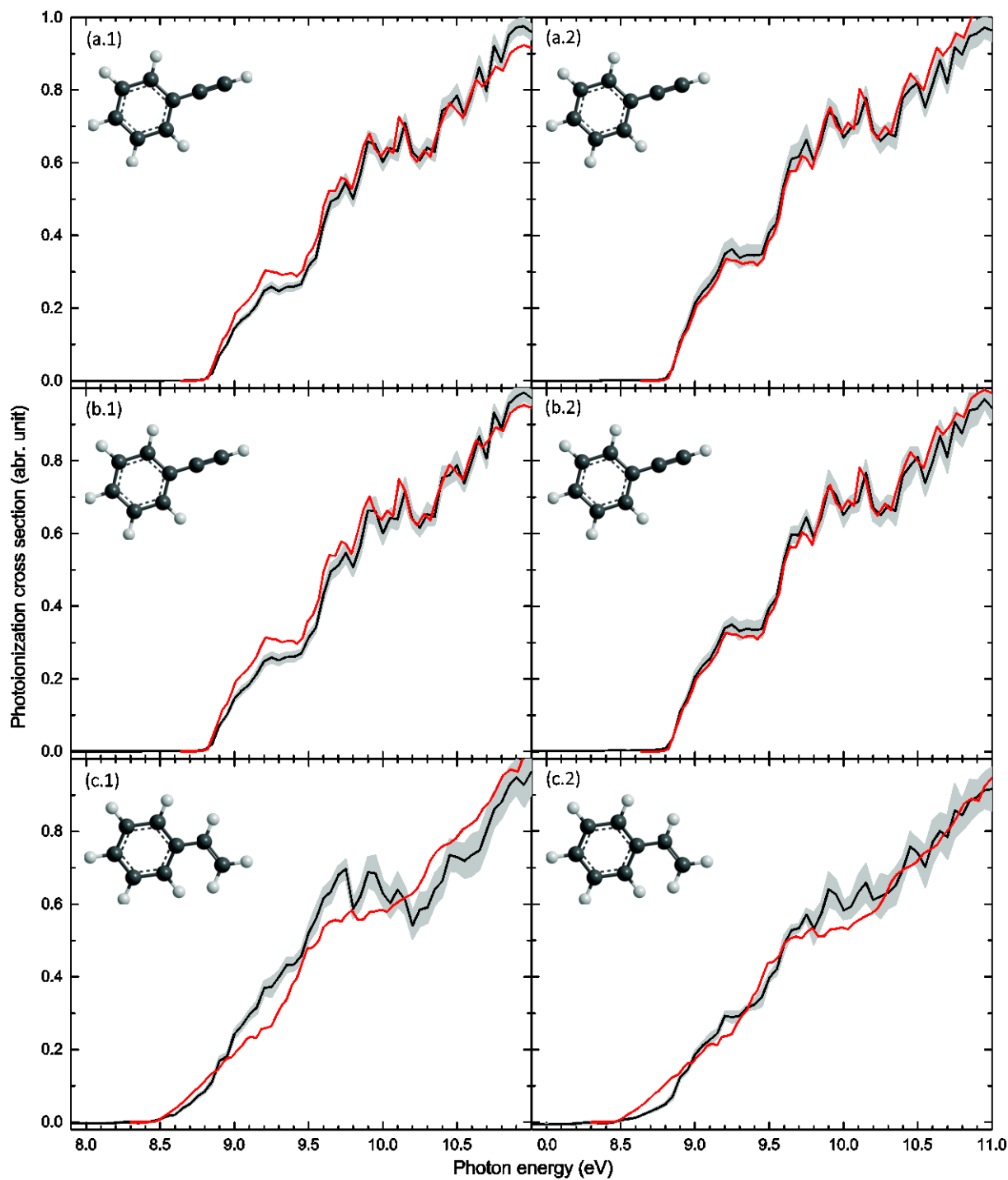


Figure S1. Photoionization efficiency curves recorded at m/z 102 (a.1), 103 (b.1) and 104 (c.1) in the helium-seeded β -bromostyrene system, and those recorded at m/z 102 (a.2), 103 (b.2) and 104 (c.2) in the acetylene-seeded β -bromostyrene system. The black lines show the experimental curves with the errors defined as the gray areas. The red lines indicate the theoretical PIE curves for phenylacetylene^[31] (a), ¹³C-phenylacetylene^[31] (b) and styrene^[31] (c).

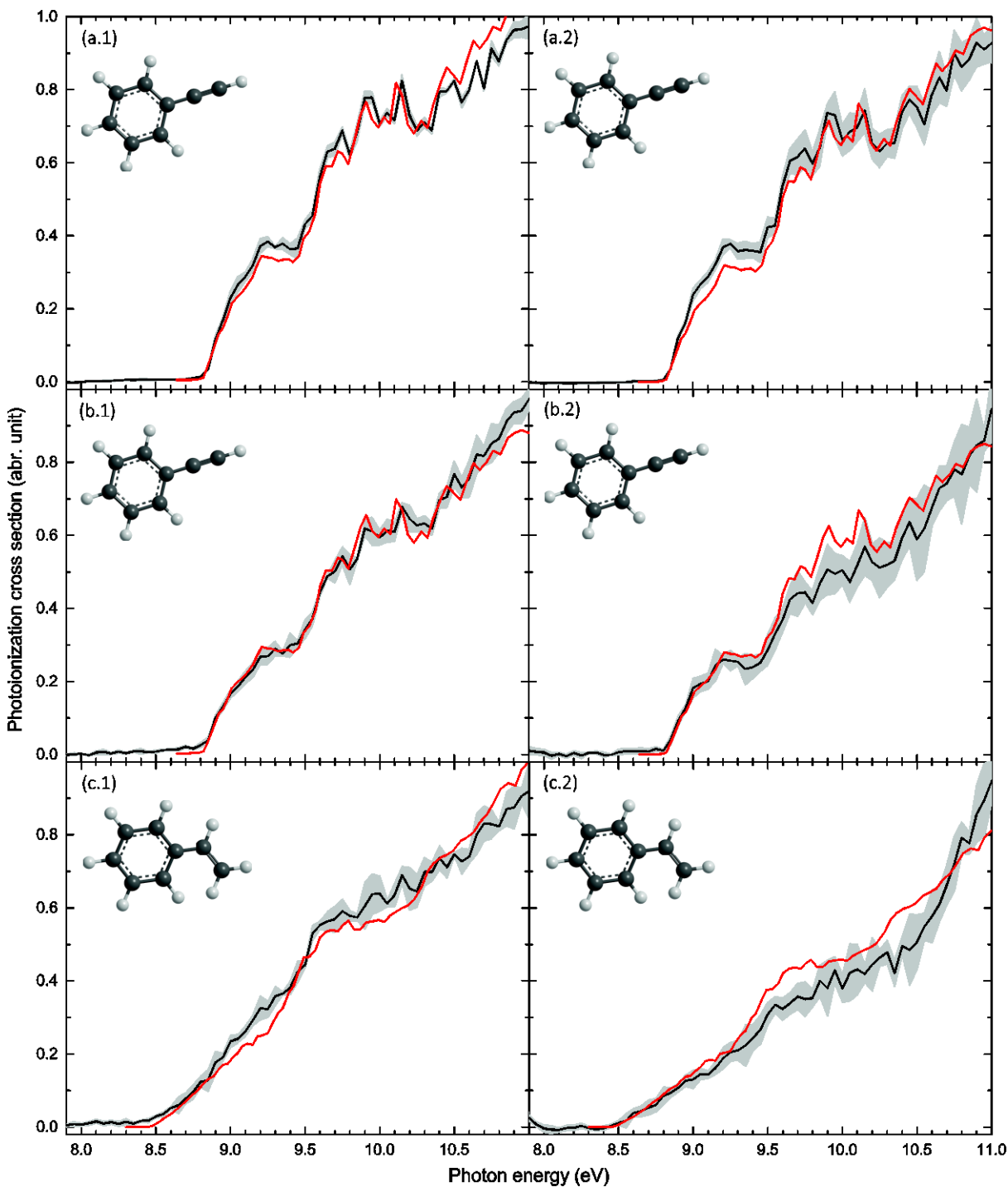


Figure S2. Photoionization efficiency curves recorded at m/z 102 (a.1), 103 (b.1) and 104 (c.1) in the helium-seeded 2-bromostyrene system, and those recorded at m/z 102 (a.2), 103 (b.2) and 104 (c.2) in the acetylene-seeded 2-bromostyrene system. The black lines show the experimental curves with the errors defined as the gray areas. The red lines indicate the theoretical PIE curves for phenylacetylene^[31] (a), ¹³C-phenylacetylene^[31] (b) and styrene^[31] (c).

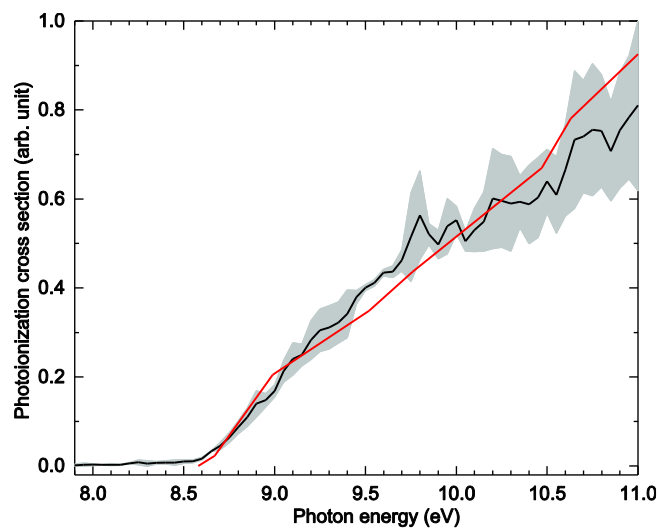


Figure S3. Photoionization efficiency curve recorded at m/z 126 in the acetylene-seeded β -bromostyrene system. The black line shows the experimental curve with the errors defined as the gray area. The red line indicates the theoretical PIE curve for 1,4-diethynylbenzene, which is the only diethynylbenzene isomer available from the database.^[4] However, the experimental PIE may be fitted by the combination of *o*-, *m*-, and *p*-diethynylbenzene isomers.

SI References

- [1] K. N. Urness, Q. Guan, A. Golan, J. W. Daily, M. R. Nimlos, J. F. Stanton, M. Ahmed, G. B. Ellison, *J. Chem. Phys.* **2013**, *139*, 124305.
- [2] Q. Guan, K. N. Urness, T. K. Ormond, D. E. David, G. B. Ellison, J. W. Daily, *Int. Rev. Phys. Chem.* **2014**, *33*, 447-487.
- [3] Z. Zhou, M. Xie, Z. Wang, F. Qi, *Rapid Commun. Mass Spectrom.* **2009**, *23*, 3994-4002.
- [4] J. Yang, Y. Li, Z. Cheng. *Photoionization Cross Section Database (Version 1.0)*, Accessed on September 16th, 2016, Center for Advanced Combustion and Energy, National Synchrotron Radiation Laboratory, Hefei, Anhui, China (2011).